# Bone-targeted extracellular vesicles from mesenchymal stem cells for osteoporosis therapy

**Yayu Wang** ( wangyayu1987@163.com )
Jinan University https://orcid.org/0000-0003-2359-537X

**Jie Yao**
Jinan University First Affiliated Hospital

**Lizhao Cai**
Jinan University First Affiliated Hospital

**Tong Liu**
Jinan University

**Xiaogang Wang**
Jinan University First Affiliated Hospital

**Ye Zhang**
Jinan University First Affiliated Hospital

**Zhiying Zhou**
Jinan University First Affiliated Hospital

**Tingwei Li**
Jinan University First Affiliated Hospital

**Minyi Liu**
Jinan University First Affiliated Hospital

**Renfa Lai**
Jinan University First Affiliated Hospital

**Xiangning Liu**
Jinan University First Affiliated Hospital

**Research**

**Keywords:** Osteoporosis, bone regeneration, stem cell derivatives, extracellular vesicles

**Posted Date:** March 31st, 2020

**DOI:** https://doi.org/10.21203/rs.3.rs-18279/v1

**Version of Record:** A version of this preprint was published at International Journal of Nanomedicine on October 1st, 2020. See the published version at https://doi.org/10.2147/IJN.S263756.

# Bone-targeted extracellular vesicles from mesenchymal stem cells for osteoporosis therapy

Yayu Wang[#1], Jie Yao[#2,3,4], Lizhao Cai[#2,3,4], Tong Liu[1], Xiaogang Wang[2,4], Ye Zhang[2,3,4], Zhiying Zhou[2,3,4], Tingwei Li[2,3,4], Minyi Liu[2,3,4], Renfa Lai[*2,3,4], Xiangning Liu[*2,3,4]

[1]Department of Cell Biology & Institute of Biomedicine, College of Life Science and Technology, Jinan University, Guangzhou, 510632, China
[2]The First Affiliated Hospital of Jinan University, Guangzhou 510630, China
[3]School of Stomatology, Jinan University, Guangzhou 510632, China
[4]Clinical Research Platform for Interdiscipline of Stomatology, Jinan University, Guangzhou 510630, China

[#]All these authors contribute equally to this work.

[*]Correspondence to Xiangning Liu

The First Affiliated Hospital of Jinan University, Guangzhou 510630, China
Phone: +86 20 3868 8109

Fax: +86 20 3868 8000

E-mail: liuxiangning2003@126.com

## Abstract

### Background

Osteoporosis (OP) is one of the most common chronic diseases, but the drugs used to treat OP have strong side effects. Recently, bone regeneration in stem cell derivatives represented by extracellular vesicles (EVs) has provided a new strategy for the prevention and treatment of OP. EVs derived from mouse mesenchymal stem cells (mMSCs) have a positive effect on bone regeneration, yet their clinical application has been hampered by the lack of bone-targeting. Alendronate (Ale) has a specifically affinity for bone tissue through a high affinity with hydroxyapatite. Herein, we used copper-free "click chemistry" to combine EVs with Ale together for OP targeted therapy. Bone targeting was facilitated via Ale binding to hydroxyapatite, which is highly expressed on the bone surface.

### Methods

*In vitro*, bone targeting of Ale-EVs was confirmed by flow cytometry. Also, *Ex vivo* fluorescent imaging data revealed strong fluorescent signals in bone tissues in mice treated with Ale-EVs-DiD compared to bone tissues of mice treated with EVs-DiD. Importantly, the modified EVs were well tolerated and showed no evidence of nonspecific side effects or immune response. Besides, our results showed that Ale-EVs could promote the proliferation and differentiation of mouse mesenchymal stem cells *in vitro.* And it had the antiosteoporotic effects in ovariectomy (OVX)-induced osteoporosis rat model.

### Conclusions

A novel bone-targeting nanoparticle delivery system was developed for osteoporosis therapy. We used the Ale-N3 to modify mMSCs derived EVs by copper-free "click chemistry" to generate a Ale-EVs system. The Ale-EVs had a high affinity for bone and have great potential for clinical applications in osteoporosis therapy with low systemic toxicity.

## Background

With the development of society and the increase of average life expectancy, osteoporosis (OP) has become one of the most common chronic diseases in today's society[1]. In the oral and maxillofacial region (OMF), OP impact the rate of alveolar bone destruction directly by changing the trabecular structure of alveolar bone[2]. Many studies have shown that OP can adversely affect the healing of mandible fractures and defects, and delay bone healing[3]. Besides, OP is closely related to the effect of dental implant restoration. It has been reported that the bone resorption around implants in OP patients is significantly higher than those with normal bone density within five years after implantation and repair. Besides, Temmerman confirmed that the five-year survival rates of implants in OP patients is lower than that in the normal group [4-6]. Therefore, effective treatment of OP can not only improve the quality and efficiency of OMF bone healing in OP patients, but also shorten the time of osseointegration.

At present, the clinical treatment drugs of OP mainly include bone resorption inhibitors (such as bisphosphonates, estrogen, selective estrogen receptor modulators and calcitonin, *etc.*); bone formation promoter (parathyroid hormone analogs, *etc.*) and other mechanisms drugs (vitamin K, active vitamin D and its analogs, *etc.*)[7-11]. As one of the bisphosphonates of bone resorption inhibitors, Alendronate (Ale) is the most widely used first-line anti-OP drug in clinical, it contains a P-C-P group of the pyrophosphate analog, which specifically binds to bone surface through a high affinity with hydroxyapatite, inhibit bone resorption by inhibiting osteoclast function. However, the drug has obvious side effects and may cause oesophagitis and gastrointestinal discomfort[12]. Therefore, it is very important to find more safe and effective methods and drugs for OP patients. With the development of regenerative medicine, the study of bone regeneration in stem cell derivatives represented by EVs has provided a new idea for the prevention and treatment of OP.

Extracellular vesicles (EVs) consist of a lipid bilayer membrane containing various proteins, RNA, and DNA. There are subpopulations of EVs including apoptotic bodies (1,000–5,000 nm), intermediate-sized microvesicles (200–1,000 nm), and exosomes (30–150 nm). The best studied of these are exosomes which are released by most cell types[13-15]. Exosomes participate in a variety of physiological and pathological processes, such as the transfer of proteins, lipids, and RNA between cells, angiogenesis, tissue regeneration, and regulating wound healing by carring biologically active molecules such as proteins and lipids, as well as mRNA and microRNA. Hu’s team studied the therapeutic potential of EVs in umbilical cord blood for elderly OP, the results showed that intravenous injection of EVs for 2 months could reduce bone loss in elderly mice. Computed tomography (CT) results showed an increment of trabecular and cortex bone mass[16]. There are also reports showed that EVs secreted by mesenchymal stem cells (MSCs) had good potential and great application value for the treatment of OP[17]. However, natural EVs lacks bone-targeting, which greatly limits its clinical application. So, how to effectively use EVs to promote osteogenesis and improve its bioavailability is an important research direction.

Bone-targeting drug molecules can confer drug carrier to target bone. However, it is difficult to gently couple these bone-targeted small molecule drugs to the surface of drug carriers.

As an efficient and gentle coupling method, "Click chemistry" can solve this problem well[18]. The "click chemical " reaction is mild, easy to operate and easy to purify products with no harmful by-products and has been widely used in surface modification, synthesis of functional polymers, cell markers, and biomedical synthesis[19]. Stefanucci Azzurra's team reported a new enkephalin analogue with great analgesic mediated by "click chemistry" [20]; Lee's team used copper-free "click chemistry" to combine growth factors with collagen together [21]. "Click chemistry" is a powerful synthetic tool in the discovery of new drugs[22]. In this study, we modified the Ale molecule with an azide group (N3), and modified the membrane surface of EVs with an alkynyl (DBCO) group using a commercial linker. Then, Ale-N3 and EVs-DBCO were coupled by "click chemistry". Finally, the EVs secreted by bone marrow MSCs was bone-tarteted through this reaction and the Ale-EVs complex was constructed to study the anti-osteoporosis effect (**Figure 1A**).

## Materials and methods

### Materials

50 kD ultrafiltration tube was purchased from Merck Millipore. Dynabeads® was purchased from Life Technologies. 2-(2-methoxy-4-nitrophenyl)-3-(4-nitrophenyl)-5-(2,4-disulfophenyl)-2H-tetrazolium, monosodium salt (WST-8) reduction assay kit was purchased from Dojindo Molecular Technologies. Anti-Col1 A1 (sc-293182), Anti-RUNX-2 (sc-10758) were from Santa-Cruz.

### Cells

The cell lines, mouse bone marrow mesenchymal stem cells (mMSCs), were purchased from the American Type Culture Collection(ATCC), basic medium was RPMI 1640 (Life Technologies, USA) supplemented with 10% fetal bovine serum (FBS) (Life Technologies, USA) and antibiotics. The cells were maintained in 5% $CO_2$ at 37°C.

### Synthesis of azido-Ale

Alendronate disodium salt (293 mg 1.0 mmol) (powder from lyophilization of aqueous solution of alendronic acid and 2 eq. NaOH) was dissolved in 0.1 M PBS (15 mL), pH 7.5. The aqueous solution was then cooled in an ice water bath, and a solution of azidobutyric acid NHS ester (226.2 MW) (Lumiprobe Corporation, Hunt Valley, Maryland, USA) in acetonitrile (ACN) (14 mL) was added. The resulting solution was warmed to room temperature and stirred for 2 hours. The solution was directly purified with reversed-phase high performance liquid chromatography (RP-HPLC) (Waters XTERRA Prep MS C8 OBD column, 5 µm, 19x150 mm), flow rate 10 ml/min, 214 nm UV. Buffer A: 0.1% trifluoroacetic acid (TFA)/$H_2O$, Buffer B: 0.1% TFA/ACN. Gradient: 100% buffer A, run 6 min; 100% buffer B, 1 min; 100% buffer B, 5 min. 100% buffer A, 1 min. 100% buffer A, 5 min. The collected eluent was lyophilized to give product as a colorless (or off-white) solid. The identity of the product was verified by Orbi-trap ESI MS (negative mode): Found 359.05 (M-H)-. Calculated: 359.05 (M-H)-.

### Isolation and purification of EVs

The MMSCs were cultured in RPMI 1640 (Life Technologies, USA) supplemented with 10% FBS and antibiotics. To remove most of the EVs present in the FBS, it was spun at 100,000 g for 60 minutes before adding to RPMI 1640. The cell culture medium was changed every two days. The cell culture medium was harvested, and centrifuged at 300 g for 15 min to discard the dead cells, impurities and other sediments. The BMSCs supernatant was centrifuged at 2000g g for 15 min to collect the supernatant again. The supernatant collected for the second time was divided into closed centrifuge tubes, equilibrated and placed in a high-speed centrifuge at 10,000 g for 2 hours to collect the supernatant. At last, The BMSCs supernatant was centrifuged at 100000 g for 70 min to collect the supernatant again. At this point, the sediment is the target material we need to collect. The supernatant was discarded and the purified EVs were resuspended in PBS buffer and stored at −80°C.

### Synthesis and characterization of Ale-EVs

Ale-EVs was synthesized through conjugation of Ale-N3 to EVs-DBCO via Copper catalyzed acetylene - azide cycloaddition reaction. First, DBCO-PEG4-NHS ester was used to add DBCO functional group to EVs' surface. Take a 1ml EP tube, add a freshly prepared alkaline PBS solution with a pH of 8.8, and add the appropriate amount of DBCO-

PEG4-NHS ester solution and EVs solution at a molar ratio of 10: 1, and incubate overnight at room temperature in the dark and spin. After rotating the sample overnight, the EVs and DBCO are coupled to form an EVs-DBCO compound. The EVs-DBCO was placed in a 50KD ultrafiltration tube and centrifuged at 10000 g for 30 minutes. After centrifugation, discard free DBCO-PEG4-NHS ester molecules and collect EVs-DBCO compounds. Dilute EVs-DBCO solution with PBS solution, and add Ale-N3 solution at a molar ratio of 10: 1 to EVs for incubating overnight at room temperature in the dark and spin. After overnight, the solution was removed into the 50KD ultrafiltration tube and centrifuged at 10000 g for 30 minutes to remove the uncoupled small molecules and to obtain the compound Ale-EVs.

**Transmission electron microscopy**

15 μg of Ale-EVs were fixed with 4% paraformaldehyde for 30 minutes at room temperature, treated in an ultrasonic bath for 2 minutes, and then vortexed for 1 minute. Subsequently, the sample was dropped onto UV-treated EM (electron microscopy) grids and kept at room temperature for 30 minutes to dry. The samples were stained with 2% uranyl acetate for 15 minutes, the excess uranyl acetate was removed and the Ale-EVs were examined by transmission electron microscope (TEM) using Philips Tecani 10 (Philips, Eindhoven, Netherlands) at 100 kV.

***In vitro* bone targeting of Ale-EVs**

Fluorescence staining was performed in Ale-EVs and EVs. The whole experiment should be conducted at room temperature and under dark conditions. The two kinds of particles were placed in EP tube respectively, and DiD dye was added with appropriate amount to incubate for 20 min. After incubation, the supernatant was placed in a 50KD ultrafiltration tube and centrifuged at 10000 g for 30 minutes to get Ale-EVs-DiD and EVs-DiD. Equal amount of Ale-EVs or EVs combined with appropriate amount of hydroxyapatite beads for 2 hour. Then, these mixtures were centrifuged at 1500 g for 5 minutes. Discard the supernatant and resuspend the particles in PBS. Next, we repeated the centrifugation at 1500 g for 5 minutes once. Finally, the supernatant was discarded, and 300 μL of PBS was added to collect the particles at the bottom of the tube and detected by flow cytometry.

***In vivo* bone targeting of Ale-EVs**

The Ale-EVs or EVs were stained by fluorescence dye DiD. Ale-EVs-DiD (150 μg EVs) were injected intravenously into nud mice. After 6 hours, DiD fluorescence in the entire body of the mouse was acquired by In-Vivo Xtreme (Bruker, Germany). After the mouse was sacrificed, DiD fluorescence was quantified in heart, liver, lung, spleen, kidney, intestine and bone tissues. Radiant efficiency was measured using MI SE software (Bruker, Germany) and normalized by tissue volume.

**ALP staining experiment**

Alkaline phosphatase (ALP) is an important indicator for detecting osteogenic differentiation of MMSCs. In this study, different types of mixtures were used to treat MMSCs plated on cell culture plates. The ALP staining was used to test whether different groups of Ale-EVs had the ability to induce osteogenic differentiation. MMSCs were lysed and centrifuged at 12,000 g for 10 minutes, followed by ALP activity kit (Beyotime, shanghai, China). After incubation at 37°C for minutes, termination solution was added and the activity of ALP was measured at the wavelength 405nm.

**Q-PCR assay**

The samples were homogenized in Trizol Reagent (Life Technologies, USA) and the RNA was isolated and purified using the protocols provided by the manufacturer. RNA concentration was determined by the NanoDrop-2000 spectrophotometer (Thermo Scientific, USA). Reverse transcription for mRNA into cDNA was performed using Prime Script®RT reagent kit (Takara, Japan). We then performed Real-Time PCR using SYBR Prime Script RT-PCR kit (Takara, Japan). PCR primers for 18s rRNA were, Forward: GTAACCCGTTGAACCCCATT and Reverse: CCATCCAATCGGTAGTAGCG[23], those for COL1-A1 were Forward: ACATGTTCAGCTTTGTGGACC and Reverse: AGGTTTCCACGTCTCACCAT, and those for RUNX-2 were Forward: CCGAGCTACGAAATGCCTCT and Reverse: GGACCGTCCACTGTCACTTT[17]. Real-Time PCR was performed using SYBR Prime Script RT-PCR kit (Takara, Japan). All assays were performed in triplicate according to the protocols provided by the manufacturer. Relative expression was determined using comparative Ct ($2^{-\Delta\Delta Ct}$) method[24].

**Western blot analysis**

Cells were lysed in lysis buffer (50 mM Tris, pH 7.5, 250 mM NaCl, 0.1% SDS, 2 mM dithiothreitol, 0.5% NP-40, 1 mM PMSF and protease inhibitor cocktail) on ice for 30 minutes. Protein fractions were collected by centrifugation at 13,000 g at 4°C for 10 minutes and the supernatant was used for examining the protein concentration by BCA kit (Sigma-Aldrich). Samples were diluted in SDS-PAGE sample buffer and denatured for 5 minutes at 95°C. Equal amounts of the protein were subjected to SDS-PAGE and transferred to PVDF membranes. The membranes were blocked with 5% BSA and incubated with specific antibodies overnight at 4°C. Subsequently, horseradish peroxidase labeled secondary antibody was added and visualized using an enhanced ECL kit. Relative protein expression was analyzed by Image-Pro Plus software version 6.0 (Media Cybernetics, Inc., Rockville, MD, USA)

**Cell viability assay**

Cell viability was assessed by using the 2-(2-methoxy-4-nitrophenyl)-3-(4-nitrophenyl)-5-(2,4-disulfophenyl)-2H-tetrazolium, monosodium salt (WST-8) reduction assay kit according to the manufacturer's instructions. MMSCs were plated in 96-well plates at a cell density of $1.5 \times 10^3$ cells per well in 100 µL of complete medium (RPMI1640 basic medium+10% FBS). The following day, the medium was replaced with reagents and incubated for 48 hours. Subsequently, WST-8 was added to the culture for 2 hours at 37°C and absorbance of each well was measured at 450 nm wavelength by enzyme standard instrument (Thermo Scientific, USA).

**Micro-CT analysis**

All the harvested specimens were examined using a micro-CT system (µCT50; Scanco Medical, Brüttisellen, Switzerland). Briefly, 100 slices with a voxel size of 10 µm were scanned in the region of the distal femur, beginning at the growth plate and extending proximally along the femur diaphysis. Eighty continuous slices beginning at 0.1 mm from the most proximal aspect of the growth plate in which both condyles were no longer visible were selected for analysis. After 3D reconstruction, bone mineral density (BMD), bone volume fraction (BV/TV), trabecular number (Tb.N), trabecular thickness (Tb.Th) and trabecular separation (Tb.Sp) were automatically determined to confirm the osteoporotic

model, while the BMD and BV/TV values in the defect regions were used to evaluate new bone formation using the auxiliary software (Scanco).

**Statistics**

All numerical data were expressed as the Mean ± S.D. Statistical differences between two groups were determined by the Student's *t* test. $P < 0.05$ was considered statistically significant.

## Results

### Synthesis and characterization of ALE-EVs system

We isolated EVs from culture supernatants of BM-MSCs. Subsequently, we combined the N3-Ale, the targeting ligand for bone, with the EVs membrane using copper-free “click chemistry” approach. This approach was illustrated in **Figure 1A** and detailed below. First, in order to make the EVs have a DBCO functional group, the compound DBCO-PEG-NH2 was decorated on the surface of the EVs through amine group (NH2) reacting with hydroxyl group (COOH-) of EVs membrane protein. Then, the azide group (N3) modified ligand Ale **(Fig. S1, Fig. S2**) could react with the DBCO group of EVs membrane protein via copper-free “click chemistry” for targeting against bone. To confirm the successful conjugation of the the azide group (N3) with the DBCO group of the modified EVs, we used the Cy5.5-N3 to combine with DBCO group of the modified EVs. Next, we captured the Cy5.5-conjugated EVs by beads and measured fluorescence signal of the beads by co-focal fluorescence microscopy. The results showed that the beads with Cy5.5- EVs had strong red fluorescence signal, but the beads with DBCO-EVs has no fluorescence signal (**Fig. 1B**). This indicated that Cy5.5-N3 was successfully bound to the outer surface of the EVs membrane by copper-free “click chemistry” approach. So we combined the N3-Ale, the targeting ligand for bone, with the EVs membrane using the same method. The morphology of the Ale-EVs was spherical and intact as demonstrated by TEM **(Fig. 1C)**. Nanoparticle tracking analysis (NTA) revealed that Ale-EVs had a mean diameter of 136 nm **(Fig. 1D)**.

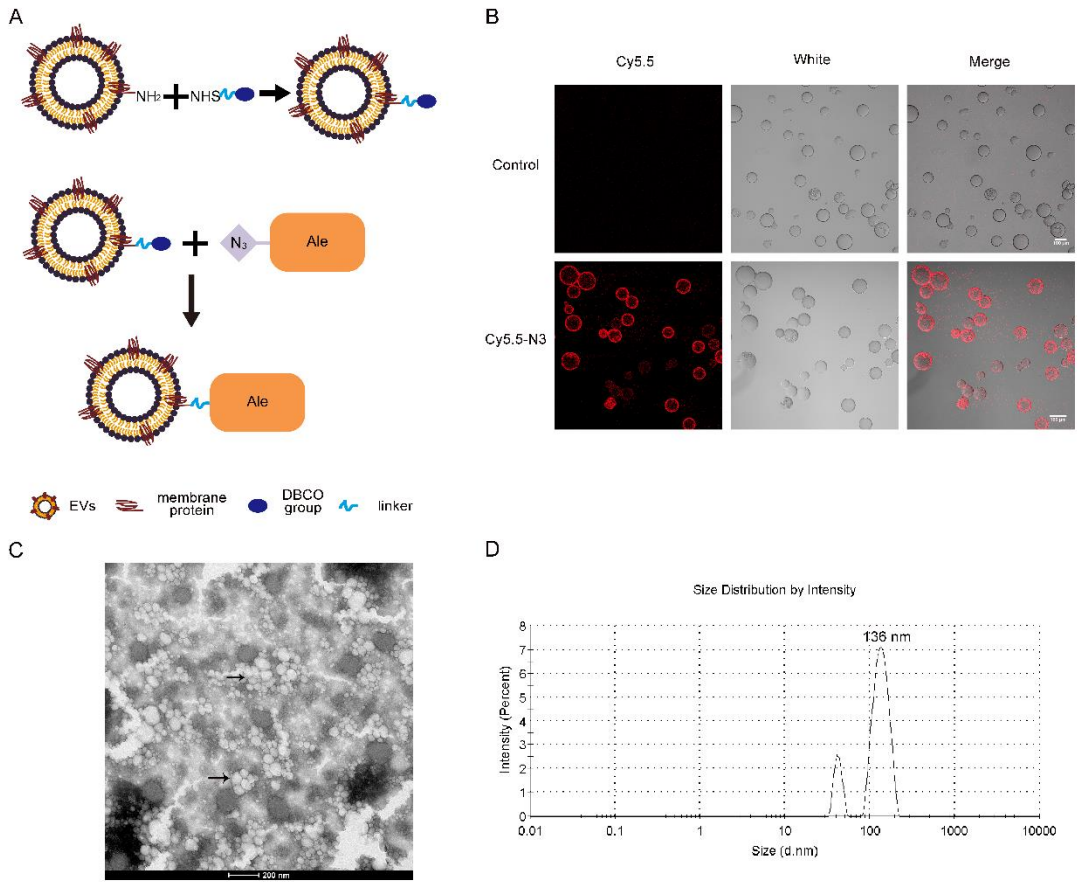

Figure 1. Synthesis and characterization of Ale-EVs.

A. Schematic illustration for synthesis of Ale-EVs.

B. Fluorescence microscopy analysis of the N3-Cy5.5 conjugation with EVs. EVs were conjugation with N3-Cy5.5 via “Click Chemistry”. Then, the Cy5.5-EVs were captured by Dynabeads® with CD63 antibody. The resulting fluorescence signal was very strong (Scale bars: 100 μm).

C. Transmission electron microscopy of Ale-EVs. The morphology of Ale-EVs was intact and the size was approximately 30-200 nm (Arrows indicate Ale-EVS, Scale bars: 200 nm).

D. Size distribution of Ale-EVs measured by nanoparticle tracking analysis. The peak diameter was at 136 nm for Ale-EVs.

**Bone targeting of Ale-EVs *in vitro* and *in vivo*.**

Ale has a high affinity with hydroxyapatite (HA), which is the main component of bone matrix. We next examined whether Ale-EVs bound to bone in a Ale-dependent manner. To determine whether Ale-EVs bound with HA beads, Ale-EVs were stained with fluorescence dye DiD (red fluorescence) and added to culture with the hydroxyapatite beads. We also used the EVs stained with fluorescence dye DiD to culture with the HA beads as a control group. As expected, flow cytometry results showed that the HA beads with Ale-EVs-DiD had a much stronger fluorescent signal than the HA beads with DBCO-EVs-DiD (**Fig. 2A**). To assess bone targeting of Ale-EVs, the Ale-EVs and EVs stained by fluorescence dye DiD were injected (iv) into mice. Mice in the control group received PBS injections (iv). Localization of Ale-EVs-DiD and EVs-DiD were monitored by *in vivo* imaging at 6 h after administration. Mice were sacrificed and then bone and other organs were harvested. *Ex vivo* fluorescent imaging data revealed strong fluorescent signals in bone tissues in mice treated with Ale-EVs-DiD compared to bone tissues of mice treated with EVs-DiD (**Fig. 2B, C**).

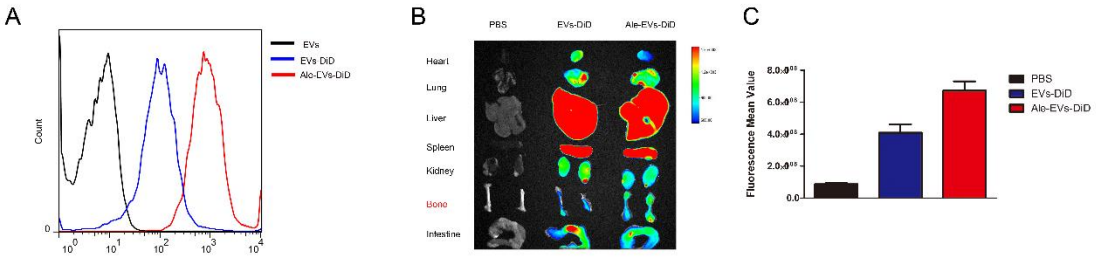


Figure 2. Bone targeting of Ale-EVs *in vitro* and *in vivo*.

A. Binding of Ale-EVs-DiD with HA beads detected by flow cytometry. Ale-EVs or EVs were loaded with DiD and then incubated with the HA beads at room temperature for 30 minutes. The result showed that the fluorescent signal was relatively stronger in HA beads incubated with Ale-EVs-DiD.

B. *Ex vivo* fluorescence imaging of major organs from mice at 6 h after intravenous injection with 150 μg of Ale-EVs-DiD, EVs-DiD or PBS. In Ale-EVs-DiD groups, bone tissues had strong fluorescence signals. In EVs-DiD groups, bone tissues had weaker fluorescence signal relatively.

C. Quantification of average fluorescence signal intensity of the bone in figure B by MI SE software. Data are presented as the mean ± s.e.m. (n=3)

**Safety of the Ale-EVs.**

We measured the *in vivo* toxicity of the Ale-EVs, especially with regard to cardiac, hepatic

and renal damage. Mice were injected with PBS or Ale-EVs (150 μg EVs per dose, iv) every other day for 1 month. Subsequently, animals were sacrificed and heart, liver, spleen and kidney were removed and stained with hematoxylin and eosin. There was no obvious tissue damage in Ale-EVs-treated mice compared with controls (**Fig. 3A**).

Furthermore, serum collected from mice treated with PBS or Ale-EVs was assessed by testing the common cardiac damage markers, creatine kinase MB isoenzyme (CK-MB). We also measured blood urea nitrogen (BUN) for renal toxicity. All serum chemistries results of mice treated with Ale-EVs were similar to PBS group (**Fig. 3B**).

To evaluate the Ale-EVs-induced possible immune response, we measured serum-associated inflammatory cytokines such as INF-α and TNF-α in mice treated with PBS or Ale-EVs. No statistically significant differences among groups in any of the tested parameters were observed (**Fig. 3C**). Thus, our data suggested that Ale-EVs are safe for *in vivo* therapy.

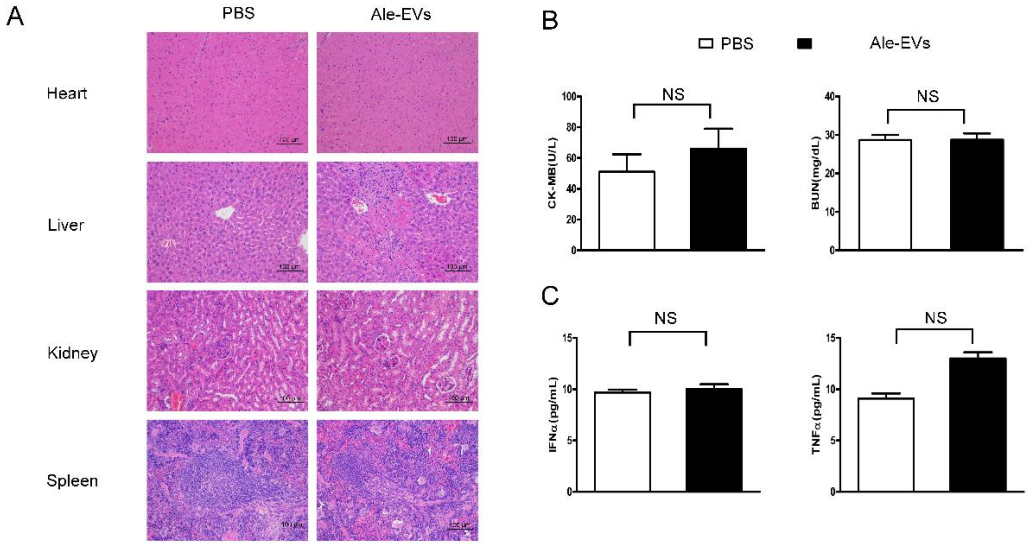


Figure 3. Evaluation of the toxicity profile of Ale-EVs.

A. H&E staining of various organs (Scale bar = 100 μm).

B. Serum markers of organ damage. Each bar represents means with SD of three replicates. NS, not significant, CK-MB: creatine kinase-MB isoenzyme; BUN: blood urea nitrogen.

C. Serum-associated inflammatory cytokines (TNF-α and INF-α). No significant difference noted between the 2 treatment groups.

### Biological function of Ale-EVs *in vitro.*

After observed with no toxicity of mice treated with Ale-EVs, we assessed whether Ale-EVs can promote the proliferation and differentiation of mouse mesenchymal stem cells (mMSCs). First, we analyzed the ability of Ale-EVs to promote mMSCs proliferation. We incubated Ale-EVs, EVs, Ale and PBS with mMSCs for 48 h following with cell viability measured with a WST-8 assay kit. Ale-EVs and EVs promoted cell proliferation compared to PBS (**Fig. 4A**). Cell growth was not promoted in the Ale-treated groups.

Next, we incubated Ale-EVs, EVs, Ale and PBS with mMSCs for 7days and 14 days respectively. And then the early marker of osteogenic differentiation was measured

by ALP activity assessment. The results showed that the OD values of Ale-EVs, EVs and Ale group were higher than the control group (**Fig. 4B**). We also assessed the levels of bone-related mRNA and protein with Q-PCR and Western blot. The results showed that the mRNA and protein expression levels of COL1 and RUNX-2 treated with Ale-EVs and EVs were remarkably up-regulated compared with the Ale and PBS groups (**Fig. 4C, D**).

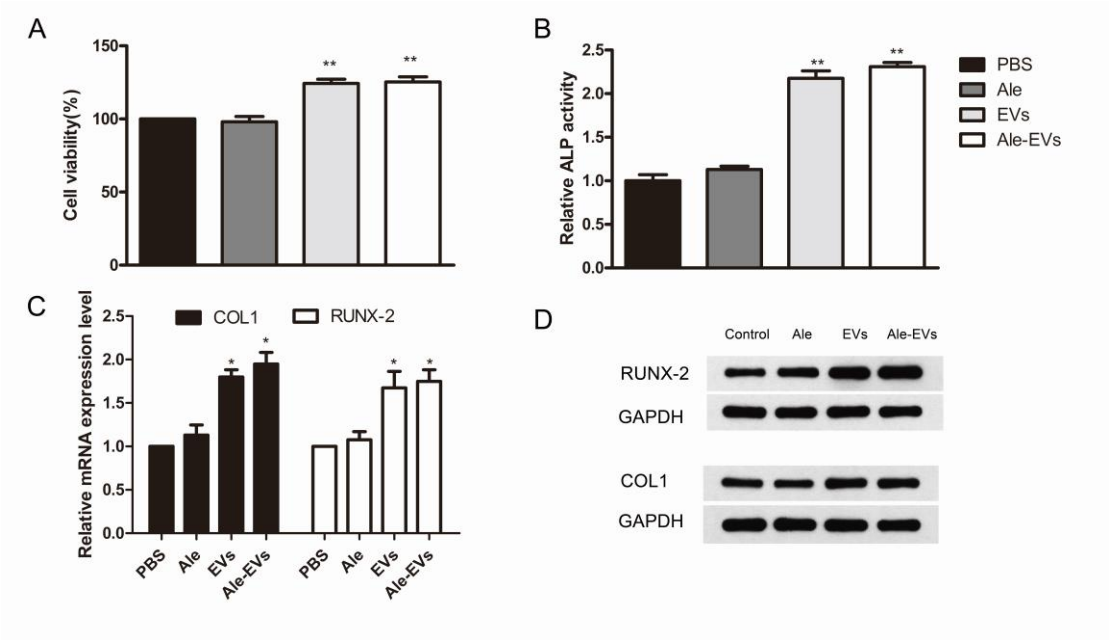


Figure 4. Antiosteoporosis efficacy of Ale-EVs *in vitro*.

MMSCs were incubated with PBS, Ale, EVs and Ale-EVs (300 μg/ml). After 48 hours, Ale-EVs and EVs promoted cells growth (A). After 14 Days, cells ALP activity were assessed using ALP staining. Ale-EVs and EVs promoted cells ALP activity remarkably, but almost had no effect in other groups(B). After 7 Days, the expression levels of RUNX-2 and COL1 were examined by (C) Q-PCR and (D) Western blot. Ale-EVs and EVs promoted the cells expression levels of RUNX-2 and COL1 remarkably.

Statistical analyses were performed using the Student's *t* test. *, $P< 0.05$； **， $P< 0.01$.

**Antiosteoporotic effects of Ale-EVs *in vivo*.**

To investigate the potential application of Ale-Evs in OP therapy, an ovariectomy (OVX)-induced osteoporosis rat model was established. Ale-Evs was then tail vein injections administered on OVX rats. The rats were randomly divided into 4 groups (n = 4 rats/group): Each group received via tail vein injections PBS, free Ale, free EVs, or Ale-EVs. Rats were treated (EVs per dose, 750 μg, iv) twice one weak for a total of 16 injections. Bone microarchitecture and BMD were measured with micro-CT. The results showed that the bone microarchitecture and bone mass was markedly better in Ale-EVs group (**Fig. 5A, B**). Moreover, analysis of BV/TV values showed that it was markedly higher in Ale-EVs group (**Fig. 5C**). The results indicated that Ale-EVs can improve bone regeneration under osteoporotic conditions.

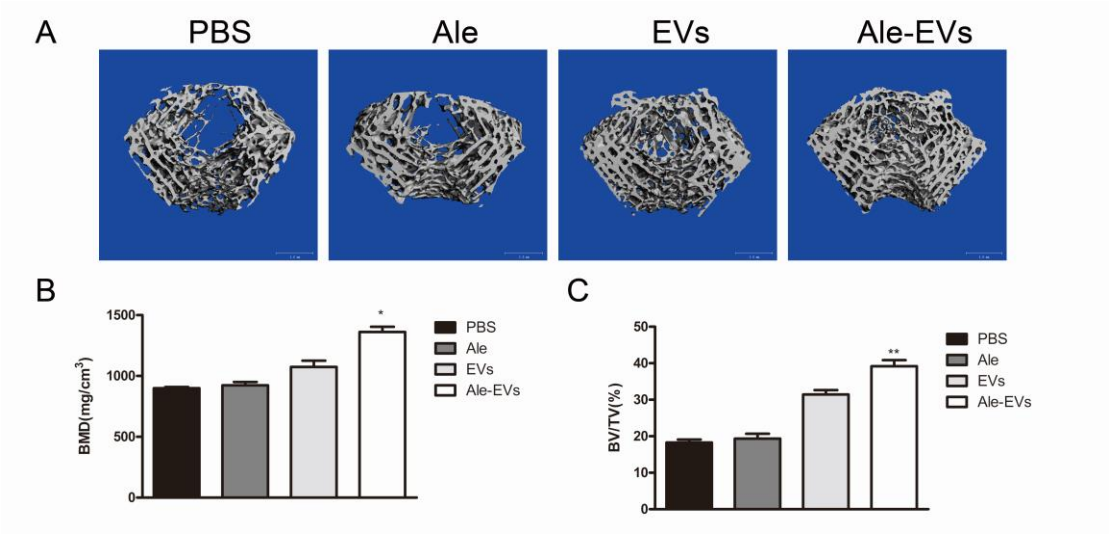


Figure 5. Antiosteoporosis efficacy of Ale-EVs *in vivo*.

A. representative images showing three-dimensional trabecular architecture by micro-CT reconstruction in distal femora (bars 1 mm);

B. micro-CT measurements of BMD in distal femora.

C. micro-CT measurements of BV/TV in distal femora.

Statistical analyses were performed using the Student's t test. *, $P< 0.05$；**，$P< 0.01$.

## Discussion

Alendronate is a bisphosphonate that combines with hydroxyapatite crystals in bone to reduce osteoclast-mediated bone resorption and reduce bone matrix destruction[12]. It has some side-effects such as osteonecrosis of the jaw[25], oral mucosa ulcerations[26], synovitis[27], arthritis[28] and GI symptoms[12]. In this study, Ale was only coupled to the surface of EVs as a bone-targeting ligand. Because of the low content of Ale coupled to the surface of EVs, its side effects were greatly reduced. Also, in the free Ale rat model control group, the anti-osteoporosis effect was not obvious due to the low content (**Fig. 5**). If we try to increase the coupling amount of Ale, it could be possible to get a better anti-osteoporosis effect of Ale-EVs.

It has been reported that MSC derived exosomes and microparticles could stimulate the repair and regeneration of tissues such as kidney, heart, and bone[29-32]. In this study, our results also showed that EVs from MMSCs could promote cell proliferation and trigger osteogenic differentiation of MMSCs *in vitro*(**Fig. 4**). It indicated that the MSCs derived EVs had the promising applications in reducing the side effects of Ale. In our study, we developed a modified EVs vesicle by conjugating alendronate to the membrane surface protein of EVs through “click chemistry” approach (**Figure 1A**), and the results provided an evidence that the vesicles could enhance bone-targeting delivery *in vitro* and *in vivo* (**Fig. 2**). By this way, we successfully combined the advantages of MSCs derived EVs and alendronate for osteoporosis therapy (**Figure 1A**). As EVs have been used as natural nano-sized vesicles for drug delivery[33], it is important to confer EVs specific tissue targeting ability. We provided a new method to modify EVs’ surface membrane for targeting ligand modification. Besides, we also could use this method to load small molecule drugs on the EVs for drug delivery.

In this study, due to the complexity of EVs and the lack of detectable markers on Ale, we cannot directly prove that Ale is coupled to the surface of EVs, nor can we calculate the amount of coupling. Therefore, we used Cy5.5-N3 to couple to the surface of EVs, it is easy to be detected because of the special fluorescent signal of Cy5.5. It proved that the compounds containing N3 groups could effectively couple with EVs-DBCO (**Fig. 1A, B**). This result indirectly proved that Ale-N3 could couple to the surface of EVs-DBCO.

At last, Ale-EVs could be used as a bone-target delivery system. We can enrich MMSCs-derived EVs with mRNAs or proteins that used to treat osteoporosis by genetic engineering technology[34-36], and strengthen the anti-osteoporosis effect of Ale-EVs. Besides, we also could load other drugs such as nucleic acid drugs [32, 37], small molecule drugs[38] into the target-delivery system to achieve the purpose of combined treatment of osteoporosis

## Conclusion

In summary, we used the bone-targeting ligand, Ale-N3, to modify mMSCs derived EVs to generate a Ale-EVs system. The Ale-EVs had a high affinity for bone and have great potential for clinical applications in osteoporosis therapy with low systemic toxicity.

## Availability of data and materials

All data generated or analyzed during this study are included in this published article.

## Authors' contributions

Yayu Wang, Renfa Lai and Xiangning Liu conceived the project. Renfa Lai and Xiangning Liu led the project and developed the reconstruction. Yayu Wang, Jie Yao, Lizhao Cai, Tong Liu, Xiaogang Wang, Ye Zhang, Zhiying Zhou, Tingwei Li and Minyi Liu performed experiments, Renfa Lai and Xiangning Liu supervised the research. Yayu Wang, Jie Yao, and Lizhao Cai analyzed the data and wrote the manuscript with the input from all the authors.


## Acknowledgements

Not applicable.

## Funding

This work was supported by Guangdong Natural Science Funds (2018A030313614); The Fundamental Research Funds for the Central Universities (21619407).


## Competing interests

Authors declare no potential conflict of interest.

## Consent for publication

All authors agree to be published.

## Ethics approval and consent to participate

Approval for the animal experiments was obtained in advance from the Animal Ethics Committee of Guangzhou Curegenix Ltd on Animal Experiments (ethical permit YSDW201812052) and all experiments in this work conform to the regulatory standards of this approval.

## Author information

Yayu Wang, Jie Yao and Lizhao Cai contributed equally to this work.


**Affiliations**

Department of Cell Biology & Institute of Biomedicine, College of Life Science and Technology, Jinan University, Guangzhou, 510632, China

Yayu Wang, Tong Liu

The First Affiliated Hospital of Jinan University, Guangzhou 510630, China
Jie Yao, Lizhao Cai, Xiaogang Wang, Ye Zhang, Zhiying Zhou, Tingwei Li, Minyi Liu, Renfa Lai, Xiangning Liu

School of Stomatology, Jinan University, Guangzhou 510632, China
Jie Yao, Lizhao Cai, Ye Zhang, Zhiying Zhou, Tingwei Li, Minyi Liu, Renfa Lai, Xiangning Liu

Clinical Research Platform for Interdiscipline of Stomatology, Jinan University, Guangzhou 510630, China
Jie Yao, Lizhao Cai, Xiaogang Wang, Ye Zhang, Zhiying Zhou, Tingwei Li, Minyi Liu, Renfa Lai, Xiangning Liu

**Corresponding author**

Correspondence to Xiangning Liu or Renfa Lai

## References

[1] Lorentzon M. Treating osteoporosis to prevent fractures: Current concepts and future developments. Journal of internal medicine. 2019;285:381-94.
[2] Ayed MS, Shafiq SS, Diab HM, Alahmari AD, Divakar DD. Assessing periapical dental radiographs as a screening parameter for early indications of osteoporosis in postmenopausal periodontal patients and root surface evaluation using spectrochemical analysis. Saudi medical journal. 2018;39:719.
[3] Tarantino U, Cerocchi I, Scialdoni A, Saturnino L, Feola M, Celi M, et al. Bone healing and osteoporosis. Aging Clin Exp Res. 2011;23:62-4.
[4] Temmerman A, Rasmusson L, Kübler A, Thor A, Merheb J, Quirynen M. A Prospective, Controlled, Multicenter Study to Evaluate the Clinical Outcome of Implant Treatment in Women with Osteoporosis/Osteopenia: 5-Year Results. Journal of dental research. 2019;98:84-90.
[5] Merheb J, Temmerman A, Rasmusson L, Kübler A, Thor A, Quirynen M. Influence of skeletal and local bone density on dental implant stability in patients with osteoporosis. Clinical implant dentistry and related research. 2016;18:253-60.
[6] Wagner F, Schuder K, Hof M, Heuberer S, Seemann R, Dvorak G. Does osteoporosis influence the marginal peri‐implant bone level in female patients? A cross‐sectional study in a matched collective. Clinical implant dentistry and related research. 2017;19:616-23.
[7] Lewis JR, Schousboe JT, Prince RL. Romosozumab versus Alendronate and Fracture Risk in Women with Osteoporosis. The New England journal of medicine. 2018;378:194-5.
[8] Fink HA, MacDonald R, Forte ML, Rosebush CE, Ensrud KE, Schousboe JT, et al. Long-Term Drug Therapy and Drug Discontinuations and Holidays for Osteoporosis Fracture Prevention: A Systematic Review. Annals of internal medicine. 2019.
[9] Naot D, Musson DS, Cornish J. The Activity of Peptides of the Calcitonin Family in Bone. Physiological reviews. 2018;99:781-805.
[10] Dempster DW, Zhou H, Ruff VA, Melby TE, Alam J, Taylor KA. Longitudinal Effects of Teriparatide or Zoledronic Acid on Bone Modeling‐and Remodeling‐Based Formation in the SHOTZ Study. Journal of Bone and Mineral Research. 2018;33:627-33.

[11] Khan M, Cheung AM, Khan AA. Drug-related adverse events of osteoporosis therapy. Endocrinology and Metabolism Clinics. 2017;46:181-92.
[12] Parker LRW, Preuss CV. Alendronate. StatPearls [Internet]: StatPearls Publishing; 2018.
[13] Théry C, Zitvogel L, Amigorena S. Exosomes: composition, biogenesis and function. Nature Reviews Immunology. 2002;2:569.
[14] Villasante A, Marturano-Kruik A, Ambati SR, Liu Z, Godier-Furnemont A, Parsa H, et al. Recapitulating the size and cargo of tumor exosomes in a tissue-engineered model. Theranostics. 2016;6:1119.
[15] Ramirez MI, Amorim MG, Gadelha C, Milic I, Welsh JA, Freitas VM, et al. Technical challenges of working with extracellular vesicles. Nanoscale. 2018;10:881-906.
[16] Hu Y, Xu R, Chen C-Y, Rao S-S, Xia K, Huang J, et al. Extracellular vesicles from human umbilical cord blood ameliorate bone loss in senile osteoporotic mice. Metabolism. 2019;95:93-101.
[17] Qi X, Zhang J, Yuan H, Xu Z, Li Q, Niu X, et al. Exosomes secreted by human-induced pluripotent stem cell-derived mesenchymal stem cells repair critical-sized bone defects through enhanced angiogenesis and osteogenesis in osteoporotic rats. International journal of biological sciences. 2016;12:836.
[18] Kacprzak K, Skiera I, Piasecka M, Paryzek Z. Alkaloids and isoprenoids modification by copper (I)-catalyzed Huisgen 1, 3-dipolar cycloaddition (click chemistry): Toward new functions and molecular architectures. Chemical reviews. 2016;116:5689-743.
[19] Thirumurugan P, Matosiuk D, Jozwiak K. Click chemistry for drug development and diverse chemical–biology applications. Chemical reviews. 2013;113:4905-79.
[20] Stefanucci A, Lei W, Pieretti S, Novellino E, Dimmito MP, Marzoli F, et al. On resin click-chemistry-mediated synthesis of novel enkephalin analogues with potent anti-nociceptive activity. Scientific reports. 2019;9:5771.
[21] Lee HJ, Fernandes-Cunha GM, Putra I, Koh W-G, Myung D. Tethering growth factors to collagen surfaces using copper-free click chemistry: surface characterization and in vitro biological response. ACS applied materials & interfaces. 2017;9:23389-99.
[22] Schwarzenböck C, Nelson PJ, Huss R, Rieger B. Synthesis of next generation dual-responsive cross-linked nanoparticles and their application to anti-cancer drug delivery. Nanoscale. 2018;10:16062-8.
[23] Zhang H, Sun Z, Wei W, Liu Z, Fleming J, Zhang S, et al. Identification of serum microRNA biomarkers for tuberculosis using RNA-seq. PloS one. 2014;9.
[24] Yuan JS, Reed A, Chen F, Stewart CN. Statistical analysis of real-time PCR data. BMC bioinformatics. 2006;7:85.
[25] Reid IR, Bolland MJ, Grey AB. Is bisphosphonate-associated osteonecrosis of the jaw caused by soft tissue toxicity? : Elsevier; 2007.
[26] Gonzalez‐Moles MA, Bagan‐Sebastian JV. Alendronate‐related oral mucosa ulcerations. Journal of oral pathology & medicine. 2000;29:514-8.
[27] Jones DPG, Savage RL, Highton J. Alendronate-induced synovitis. The Journal of rheumatology. 2008;35:537-8.
[28] Diaz-Borjon A, Seyler TM, Chen NL, Lim SS. Bisphosphonate-associated arthritis. JCR: Journal of Clinical Rheumatology. 2006;12:131-3.
[29] Wang R, Lin M, Li L, Qi G, Rong R, Xu M, et al. Bone marrow mesenchymal stem cell-derived exosome protects kidney against ischemia reperfusion injury in rats. Zhonghua yi xue za zhi. 2014;94:3298-303.

[30] Zhang J, Guan J, Niu X, Hu G, Guo S, Li Q, et al. Exosomes released from human induced pluripotent stem cells-derived MSCs facilitate cutaneous wound healing by promoting collagen synthesis and angiogenesis. Journal of translational medicine. 2015;13:49.
[31] Narayanan R, Huang C-C, Ravindran S. Hijacking the cellular mail: exosome mediated differentiation of mesenchymal stem cells. Stem cells international. 2016;2016.
[32] Nie H, Xie X, Zhang D, Zhou Y, Li B, Li F, et al. Use of lung-specific exosomes for miRNA-126 delivery in non-small cell lung cancer. Nanoscale. 2020.
[33] Vader P, Mol EA, Pasterkamp G, Schiffelers RM. Extracellular vesicles for drug delivery. Adv Drug Deliver Rev. 2016;106:148-56.
[34] Zhuang M, Chen X, Du D, Shi J, Deng M, Long Q, et al. SPION decorated exosome delivery of TNF-α to cancer cell membranes through magnetism. Nanoscale. 2020;12:173-88.
[35] Yang Z, Shi J, Xie J, Wang Y, Sun J, Liu T, et al. Large-scale generation of functional mRNA-encapsulating exosomes via cellular nanoporation. Nature Biomedical Engineering. 2020;4:69-83.
[36] Hall J, Prabhakar S, Balaj L, Lai CP, Cerione RA, Breakefield XO. Delivery of therapeutic proteins via extracellular vesicles: review and potential treatments for Parkinson's disease, glioma, and schwannoma. Cellular and molecular neurobiology. 2016;36:417-27.
[37] Zhang G, Guo B, Wu H, Tang T, Zhang B-T, Zheng L, et al. A delivery system targeting bone formation surfaces to facilitate RNAi-based anabolic therapy. Nature medicine. 2012;18:307.
[38] Higdon K, Scott A, Tucci M, Benghuzzi H, Tsao A, Puckett A, et al. The use of estrogen, DHEA, and diosgenin in a sustained delivery setting as a novel treatment approach for osteoporosis in the ovariectomized adult rat model. Biomedical Sciences Instrumentation. 2001;37:281-6.

# Figures

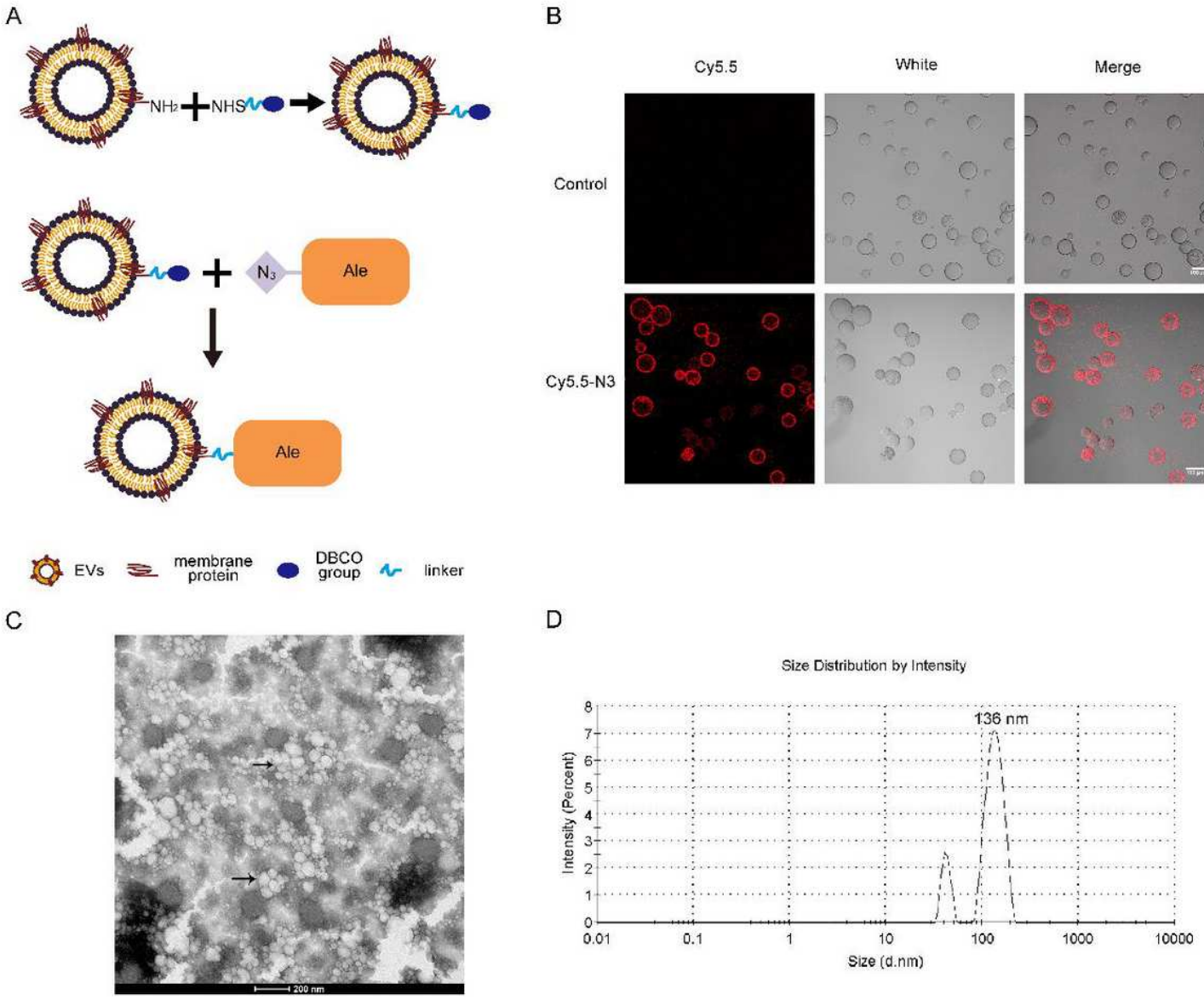


**Figure 1**

S ynthesis and characterization of Ale EVs . A. Schematic illustration for synthesis of Ale EVs. B. Fluorescence microscopy analysis of the N3 Cy5.5 conjugation with EVs. EVs were conjugation with N3 Cy5.5 via “Click Chemistry”. Then, the Cy5.5-EVs were captured by Dynabeads® with CD63 antibody. The resulting fluorescence signal was very strong (Scale bars: 10 0 μm μm). C. Transmission electron microscopy of A le EVs . The morphology of A le EVs was intact and the size was approximately 30 2 00 nm (Arrows indicate A le EVS , Scale bars: 2 00 nm). D. Size distribution of Ale EVs measured by nanoparticle tracking analysis. The peak diameter was at 136 nm for Ale EVs.

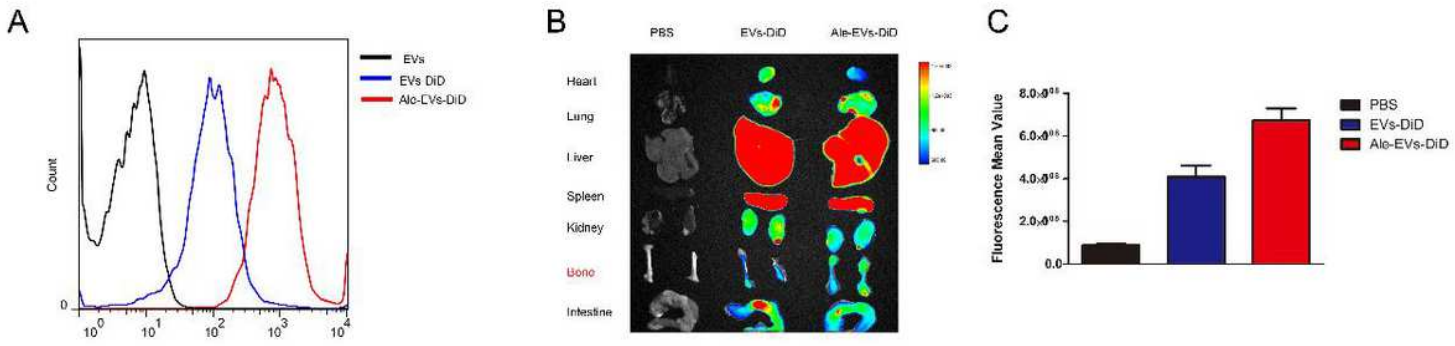


## Figure 2

B one targeting of Ale EVs in vitro and in vivo A. Binding of Ale EVs Di D with HA beads detected by flow cytometry Ale EVs or EVs were loaded with Di D and then incubated with the HA beads at room temperature for 30 minutes. The result showed that the fluorescent signal was relatively stronger in HA beads incubated with Ale EVs Di D B. Ex vivo fluorescence imaging of major organs from mice at 6 h after intravenous injection with 15 0 μg of A le EVs Di D EVs Di D or PBS. In A le EVs Di D group s , bone tissue s had strong fluorescence signals In EVs Di D group s , bone tissue s had weak er fluorescence signal relatively C. Quantification of average fluorescence signal intensity of the bone in figure B by MI SE software Data are presented as the mean ± s.e.m. (n=3)

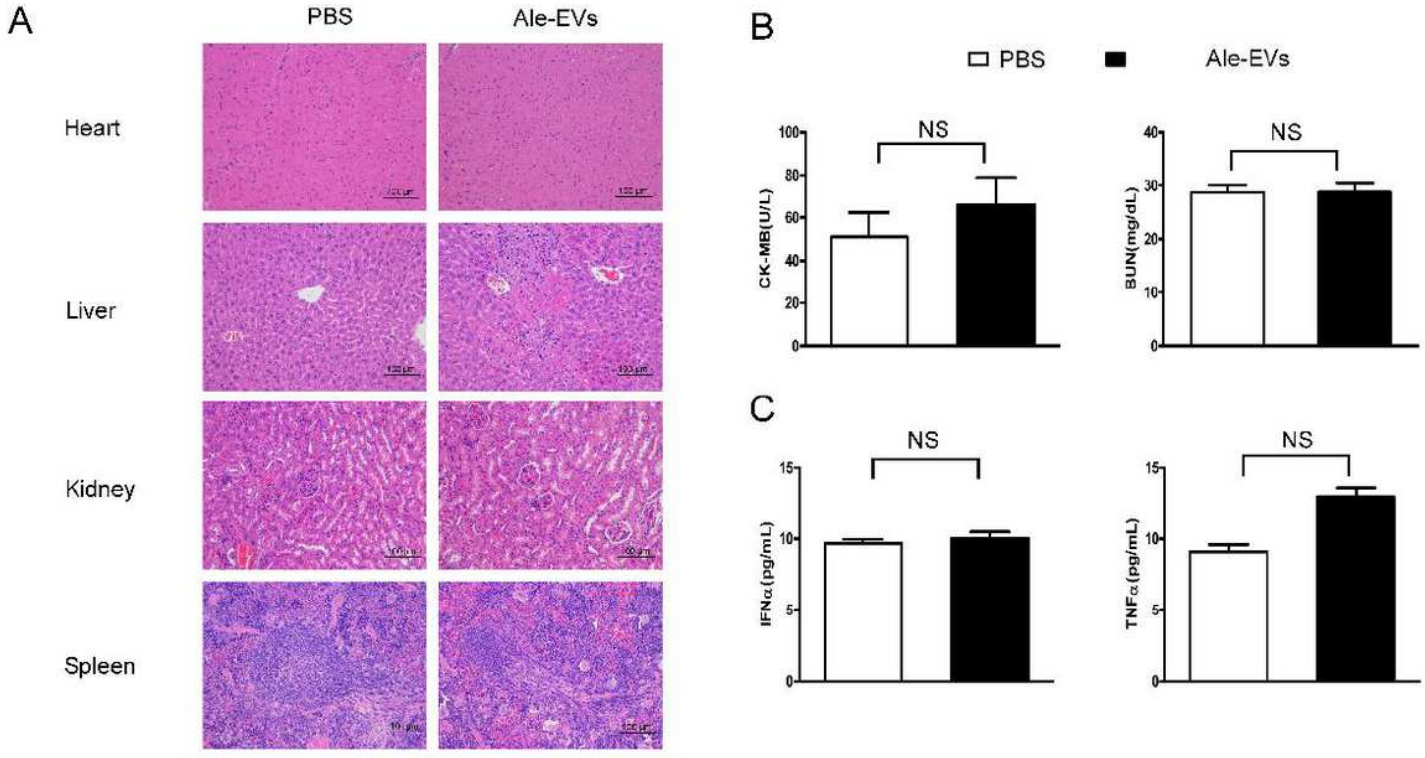


## Figure 3

Evaluation of the toxicity profile of Ale EVs A. H&E staining of various organs Scale bar = 100 μm B. Serum markers of organ damage. Each bar represents means with SD of three replicates. NS, not

significant, CK MB: creatine kinase MB isoenzyme BUN: blood urea nitrogen. C. Serum associated inflammatory cytokines (TNF α and INF α). No significant difference note d between the 2 treatment groups.

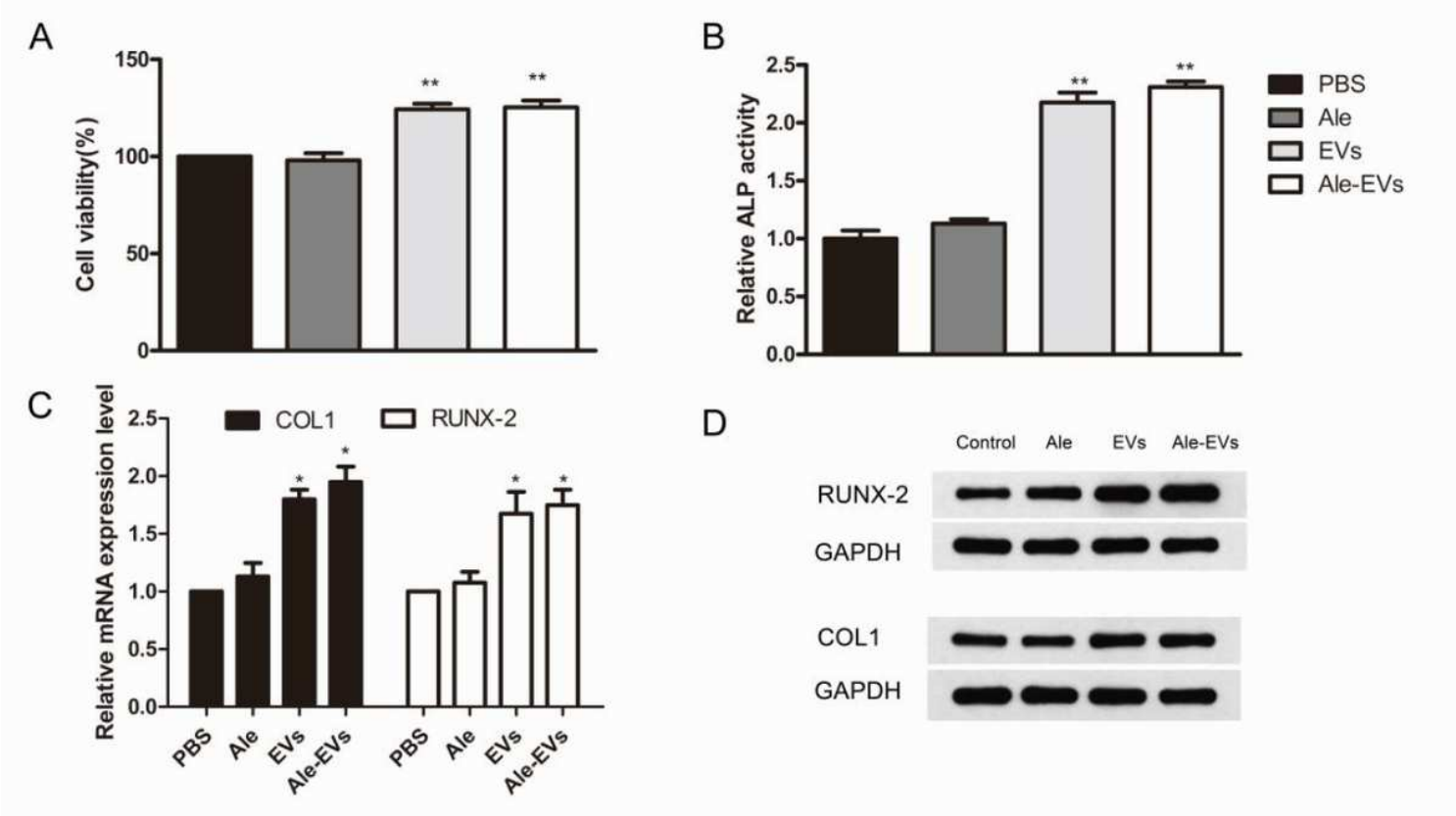


## Figure 4

Antiosteoporosis efficacy of Ale EVs in vitro MMSC s were incubated with PBS, Ale , EVs and A le EVs ( 3 0 0 μg /ml ). After 48 hours, Ale EVs and EVs promoted cells growth ( A). After 14 Days, c ell s ALP activity were assessed using ALP staining A le EVs and EVs promoted c ell s ALP activity remarkably, but almost had no effect in other groups (B After 7 Days, the expression levels of RUNX 2 and COL1 were examined by ( C ) Q PCR and ( D ) Western Ale EVs and EVs promoted the c ell s expression levels of RUNX 2 and COL1 remarkably Statistical analyses were performed using the Student's t test. *, P < 0.05; **, P<0.01

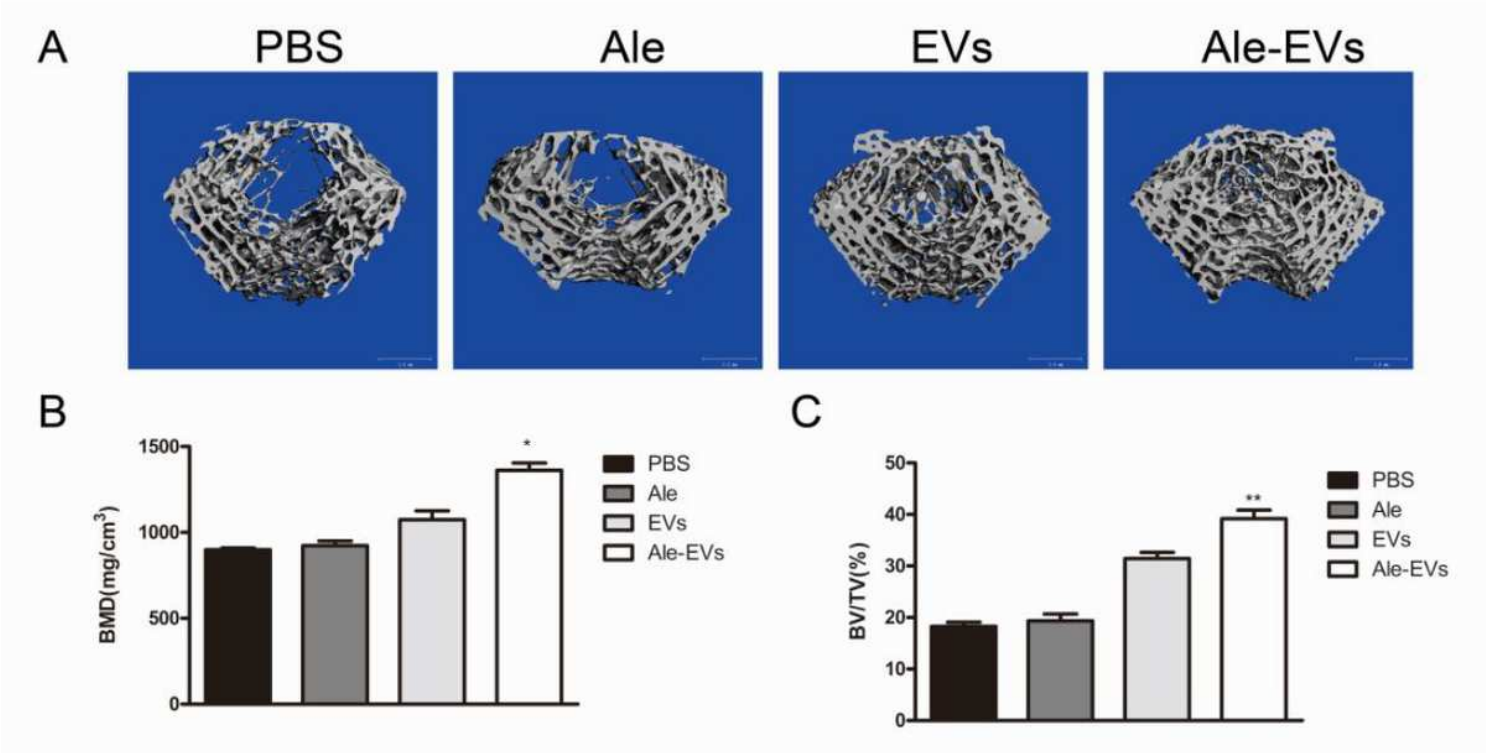


**Figure 5**

Antiosteoporosis efficacy of Ale EVs in vivo A. representative images showing three dimensional trabecular architecture by micro CT reconstruction in distal femora (bars 1 mm); B. micro CT measurements of BMD in distal femora . C. micro CT measurements of BV/TV in distal femora Statistical analyses were performed using the Student's t test. *, P< 0.05; **, P< 0.01.

## Supplementary Files

This is a list of supplementary files associated with this preprint. Click to download.

- Supplementarydata.pdf